Chapter 1

Introduction

1.1 Phase mixing

Weakly collisional plasmas are quite common in nature—the solar wind, the interstellar medium, the core of fusion devices like tokamaks being a few examples of such plasmas. Since collisions are rare, the particle velocity distribution functions $f(v)$ of these plasmas are not necessarily Maxwellian. Hence, a kinetic description that evolves $f(v)$ may be required to describe some phenomena accurately.

One of the most important features of these systems is Landau damping, a property of weakly collisional plasmas whereby waves in the plasma get damped as non-Maxwellian structure in the distribution function is generated. In his original paper, Landau [4] considered the longitudinal electron oscillations [5] in the collisionless limit as an initial value problem, and solved it using a Laplace transform technique. A different approach was used by Van Kampen [6], in which he solved the same problem by means of a normal mode expansion, and found a larger set of solutions (beyond the ones that satisfy the dispersion relation). Case [7] demonstrated the equivalence of these two approaches*, and showed that Landau damping is fundamentally a phase mixing process, where a plane wave perturbation, written as a linear combination of the eigenmodes, is damped due to the systematic

*He modified the Landau approach slightly, in order to derive the full set of Van Kampen's solutions.

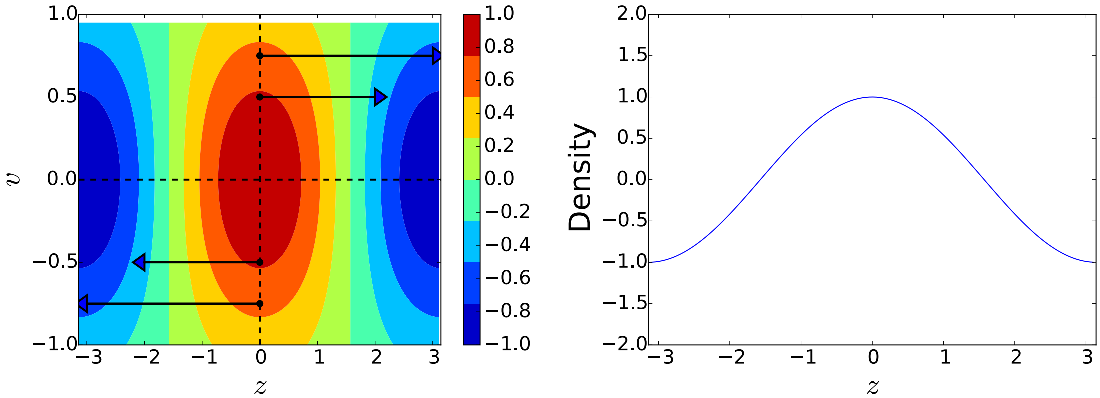

Figure 1.1: The initial perturbed distribution function (left), and the corresponding density perturbation (right).

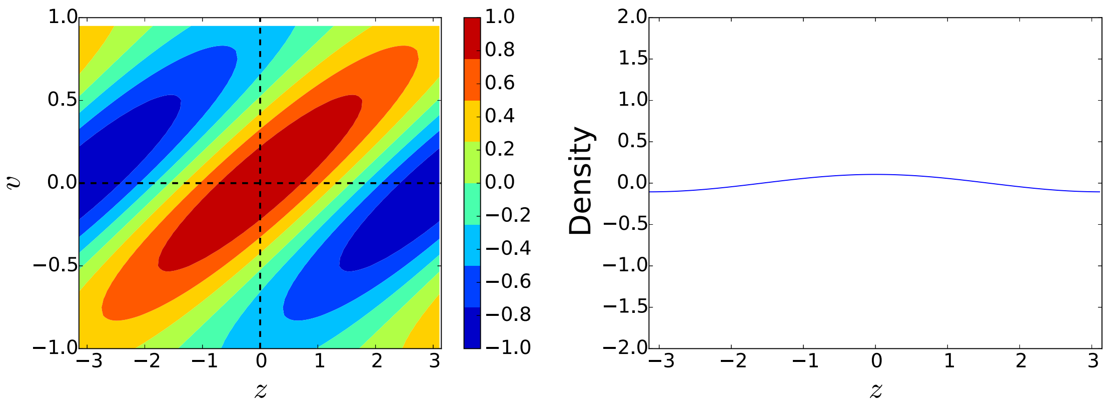

Figure 1.2: The perturbed distribution function (left), and the corresponding density perturbation (right) at time t.

smearing of the normal modes.

For a simple illustration of phase mixing, consider a homogeneous 1D plasma in equilibrium, with a perturbed ion distribution function δf:

$$\delta f(z, v, t = 0) = \cos(kz) F_0(v). \tag{1.1}$$

Here, the perturbation is assumed to be a cosine in the spatial direction z, and

Maxwellian in velocity space, $F_0(v) = \exp\left(-v^2/v_{\rm th}^2\right)/\sqrt{\pi}v_{\rm th}$, where $v_{\rm th} = \sqrt{2T/m}$ is the thermal velocity of the ions, T is the ion temperature, and m is the ion mass. This perturbed distribution function corresponds to a density perturbation δn:

$$\delta n(z, t = 0) = \cos(kz), \tag{1.2}$$

where $\delta n = \int dv\, \delta f$. The initial condition given by Eqs. (1.1–1.2) is plotted in Fig. 1.1. Ignoring electromagnetic effects, as time evolves, ions with different velocities move to different locations in space, generating structure in the perturbed distribution function with respect to v at a constant z:

$$\delta f(z, v, t) = \cos(kz - kvt)F_0(v). \tag{1.3}$$

Since density is the integral of the distribution function over velocity ($\delta n = \int dv\, \delta f$), as the distribution function becomes more and more striated, the density diminishes:

$$\delta n(z, t) = \cos(kz) \exp\left(-k^2 v_{\rm th}^2 t^2/4\right). \tag{1.4}$$

The perturbed distribution function and the perturbed density at time t are plotted in Fig. 1.2. This transfer of structure from real to velocity space, resulting in damping of low order velocity moments is known as phase mixing†.

†There is another, nonlinear, phase mixing process [8] which plays an important role in the turbulence of weakly collisionless plasmas at scales comparable to the ion Larmor radius. However, in this thesis we only consider turbulence at scales larger than the ion Larmor radius, and ignore this process. As a result, the linear phase mixing discussed here is the only phase mixing process in our models.

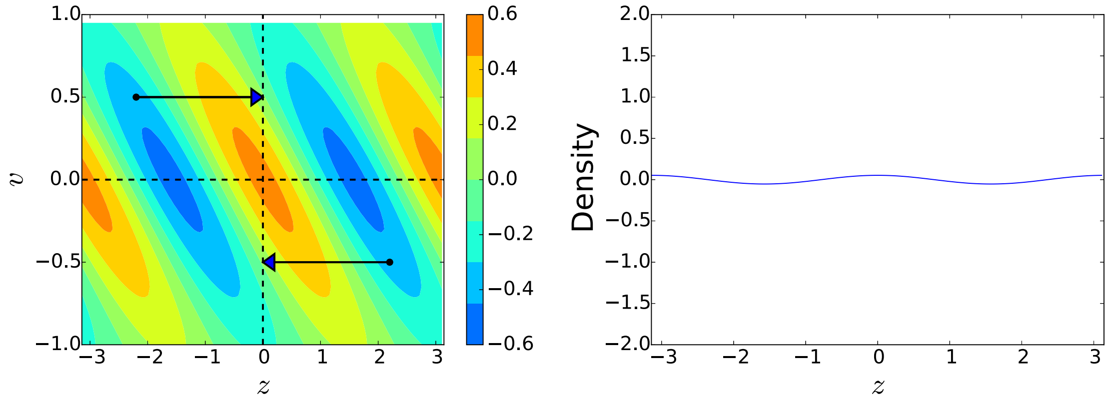

Figure 1.3: The perturbed distribution function (left), and the density perturbation (right), for a mode that is nonlinearly generated by the mode in Fig. 1.2. It is assumed that this new mode has a wavenumber p, such that $\mathrm{sgn}\,(p) = -\mathrm{sgn}\,(k)$.

In the collisionless limit, phase mixing is a reversible process. The distribution function does not "forget" the original perturbation that gets damped, and in theory, can return the system to its original state. The most famous example of such reversibility is the plasma echo [9–12]. In these experiments, a perturbation of the electric potential is excited, which Landau damps away; later, another perturbation of the electric potential is excited, which also damps away; subsequently, a non-zero electric potential perturbation (the echo) is observed to appear in the plasma. The two original electric pulses couple nonlinearly to generate this echo.

The cartoon for phase mixing discussed above (see Figs. 1.1 and 1.2) can be extended to include the echo as follows. Imagine that the perturbation shown in Fig. 1.2 nonlinearly couples with another perturbation to generate a mode which has an oppositely signed wavenumber p:

$$\delta f_{\mathrm{echo}}(z, v, t) = A \cos(pz - kvt) F_0(v), \tag{1.5}$$

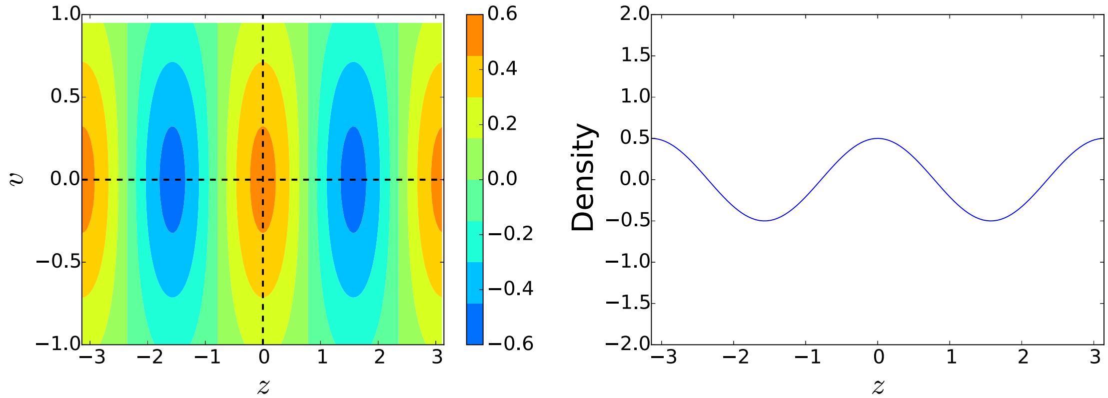

Figure 1.4: The perturbed distribution function (left), and the density perturbation (right), for the mode shown in Fig. 1.3, at a later time $t\,(1-k/p)$.

where A is the amplitude of this new perturbation. This mode corresponds to a density perturbation given by

$$\delta n_{\mathrm{echo}}(z,v,t) = A\cos(pz)\exp\left(-k^2t^2/4\right). \tag{1.6}$$

The perturbed distribution function, and the density perturbation for this mode are plotted in Fig. 1.3. Observe that due to the change in sign of the wavenumber, the phase space contours of the perturbed distribution function are now tilted in the opposite way. At a later time $t+t'$, this perturbed distribution function evolves into

$$\delta f_{\mathrm{echo}}(z,v,t+t') = A\cos(pz - pvt' - kvt)F_0(v). \tag{1.7}$$

Since p and k are oppositely signed, the corresponding density perturbation at this later time is larger than the one in Eq. (1.6):

$$\delta n_{\text{echo}}(z, v, t + t') = A \cos(pz) \exp\left(-(kt + pt')^2/4\right) . \tag{1.8}$$

This perturbation is plotted in Fig. 1.4 for time $t + t' = t\,(1 - k/p)$.

It is shown in Chapter 3 that the echo is inherently a nonlinear phenomenon, and is not observed for an isolated Fourier mode. In Chapters 4 and 5 nonlinear models are considered, where different Fourier modes are coupled to each other. Nonlinearly, the plasma echo may be observed. The necessary conditions required for an echo are discussed in detail within these chapters.

1.2 Turbulence

Turbulence is ubiquitous, yet a precise definition of turbulence does not exist. A simple picture of a turbulent system is depicted in Fig. 1.5: energy is injected into the system at some large scale, which then cascades down to smaller and smaller scales. Eventually a dissipative process like viscosity takes over and dissipates the injected energy[‡]. The driving scale and the dissipative scale need to be far removed from each other for the system to exhibit turbulence. For this to be true the ratio of the driving length scale to the dissipation length scale, also known as the Reynolds number, is required to be large—a basic requirement for turbulence.

For our purposes we broadly classify models of turbulence into two categories—

[‡] *Big whorls have little whorls that feed on their velocity, and little whorls have lesser whorls and so on to viscosity.*—Lewis F. Richardson

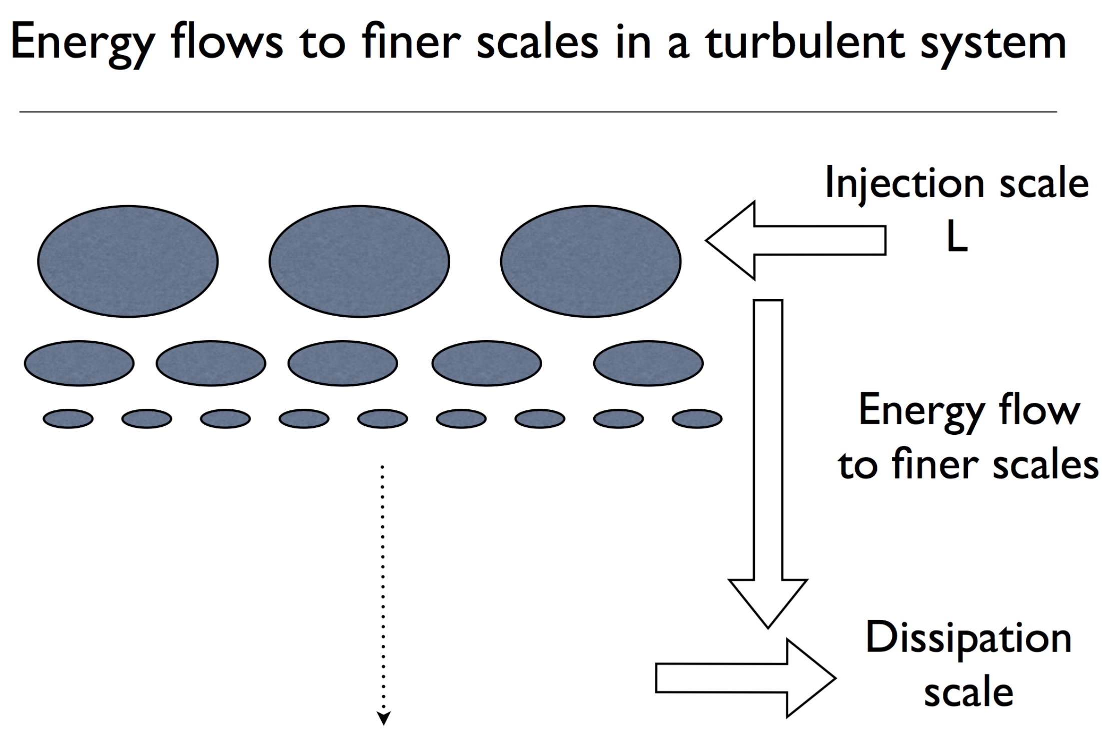

Figure 1.5: A cartoon picture of turbulence.

fluid models and kinetic models. Fluid models describe systems where the mean free path for collisions is smaller than any length scale of interest, *i.e.*, collisions are frequent. Whereas, kinetic models are applicable to systems where the mean free path is comparable to, or larger than the system size, *i.e.*, collisions are rare. Henceforth, we use the terms "fluid/kinetic model of turbulence", and "fluid/kinetic turbulence" interchangeably.

1.2.1 Fluid turbulence

One of the first theories describing turbulence in neutral fluids was by Kolmogorov [13], in which he predicts the famous $k^{-5/3}$ power law spectrum for homogeneous isotropic turbulence. In order to derive this spectrum, he made some key assumptions that have come to underlie turbulence theory: (i) statistical properties of turbulence, such as the energy spectrum, are universal at scales in between the injection and dissipation scale; (ii) the energy transfer from large to small scales happens locally in wavenumber space; (iii) no energy is lost at the intermediate scales, in other words, the flux of energy through each scale is independent of the scale.

Under these assumptions the energy density spectrum can be derived as follows: let u_λ be a velocity fluctuation at the length-scale λ. The (constant) flux of energy ϵ through the scale λ is then given by,

$$\frac{u_\lambda^2}{\tau_\lambda} \sim \epsilon, \tag{1.9}$$

where τ_λ^{-1} is the energy cascade rate at scale λ. Since the energy transfer to smaller scales is local, the cascade rate must be a function of quantities that depend on λ. Since u_λ and λ are the only physical quantities available, the cascade rate can be estimated as,

$$\tau_\lambda \sim \frac{\lambda}{u_\lambda}. \tag{1.10}$$

Therefore,

$$u_\lambda^2 \sim (\epsilon\lambda)^{2/3}. \tag{1.11}$$

Hence, the energy spectrum is a power law $k^{-\alpha}$. For $u_\lambda^2 \propto \lambda^g$, the spectral exponent α is calculated as $\alpha = g + 1$ [14]. Therefore, from Eq. (1.11), the energy spectrum for turbulence in the fluid limit is $k^{-5/3}$.

The power law spectrum is characteristic of broadband fluctuations, which may be thought of as a signature of turbulent systems.

1.2.2 Kinetic turbulence

In this section, we shall move away from the discussion about neutral fluid turbulence, and discuss the general properties of turbulence in weakly collisional plasmas. In addition to the fluid-like turbulent cascade in real space, weakly collisional systems also allow for transfer of energy to small velocity space scales by phase mixing. This makes the nature of dissipation for such systems a contentious issue [15]. Even though phase mixing damps perturbations in the plasma, the process is reversible in the collisionless limit, *i.e.*, it does not generate entropy. Therefore, phase mixing is not dissipative in the true sense. Irreversible heating for these sys-

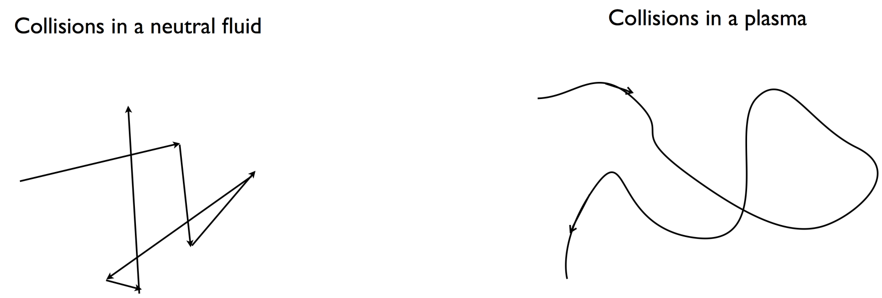

Figure 1.6: Collisions in neutral fluids (left) result in sharp changes in velocity. Whereas, a particle (ion or electron) in a plasma undergoes many small-angle collisions (right). Therefore, collisions can be modeled as a diffusive operator in the velocity co-ordinate.

tems is only possible through collisions [1,16]. Collisions in plasmas are of a different character than the ones in neutral fluids (see Fig. 1.6). Unlike neutral fluids, particles (ions or electrons) in a plasma undergo numerous long-range collisions, which individually do not alter the velocity of the particle by much. Therefore, collisions can be modeled as a diffusive operator in velocity space: $\sim \nu\,\partial_v^2$ [1,17], where ν is the frequency with which a particle velocity is changed by $\pi/2$ radians. For systems with vanishingly small ν, energy has to be transferred to small scales in velocity space, before it can dissipate via collisions. As a result, in the weakly collisional limit, the cascade of energy occurs in the phase space (real and velocity space) [1, 8, 16]—the spatial cascade is the usual fluid-like nonlinear refinement of scales, whereas the cascade in velocity space is due to phase mixing.

The systems studied in this thesis are assumed to be weakly collisional, and allow for the above mentioned phase space cascade.

1.3 Magnetized plasmas

In addition to assuming that the plasma is weakly collisional, it is also assumed to be strongly magnetized. A strongly magnetized plasma is threaded by a mean magnetic field such that the ion Larmor radius is much smaller than the system size. Additionally, it is assumed that the magnitude of the background magnetic field is much larger than the turbulent electromagnetic fluctuations. For magnetic confinement fusion devices, this is a given, as a guide field is necessary for confinement of the burning plasma. For space and astrophysical plasmas, the large scale magnetic fluctuations behave as a background magnetic field for the small scale turbulence (Kraichnan hypothesis [18]).

The background magnetic field makes these systems very anisotropic [19,20]—the perpendicular length scales (λ) are much smaller than the parallel length scales (l). For such anisotropic systems, the Kolmogorov derivation for the energy spectrum is no longer possible, since the timescale at a given scale cannot be determined uniquely. There is a perpendicular, nonlinear timescale λ/u_λ, and a parallel, linear timescale associated with the Alfvén waves l/v_A, where v_A is the Alfvén velocity. In the magnetohydrodynamic limit, Goldreich and Sridhar [19, 20] proposed a way forward by assuming that the turbulence, at sufficiently small scales, arranges itself in such a way that the linear and nonlinear timescales are comparable to each other [21, 22]. This assumption, taken scale by scale is known as *critical balance.*

One can then estimate the cascade time as

$$\tau_\lambda \sim \frac{\lambda}{u_\lambda} \sim \frac{l}{v_A}, \tag{1.12}$$

which once again gives,

$$u_\lambda \sim (\epsilon\lambda)^{1/3}. \tag{1.13}$$

This again corresponds to a $k_\perp^{-5/3}$ spectrum, but now the spectrum is in the perpendicular direction, as opposed to the isotropic spectrum derived earlier for neutral fluids. The critical balance assumption also relates the parallel and perpendicular length scales:

$$l \sim l_0^{1/3}\lambda^{2/3}, \tag{1.14}$$

where $l_0 = v_A^3/\epsilon$; l_0 is the parallel length scale where the velocity fluctuation is comparable to the Alfvén velocity, and can be thought of as a natural outer scale. Therefore, the velocity fluctuation scaling with respect to l is given by

$$u_\lambda \sim \left(\frac{\epsilon^{1/3}}{l_0^{1/6}}\right) l^{1/2}. \tag{1.15}$$

This corresponds to a parallel spectrum of $k_\parallel^{-2}$. The relationship given by Eq. (1.14) between the parallel and perpendicular length scales looks like $k_\parallel \sim k_\perp^{2/3}$ in terms of the wavenumbers, *i.e.*, as the cascade moves forward to smaller spatial scales, it gets increasingly anisotropic.

In addition to the spatial scale separation, the background magnetic field also

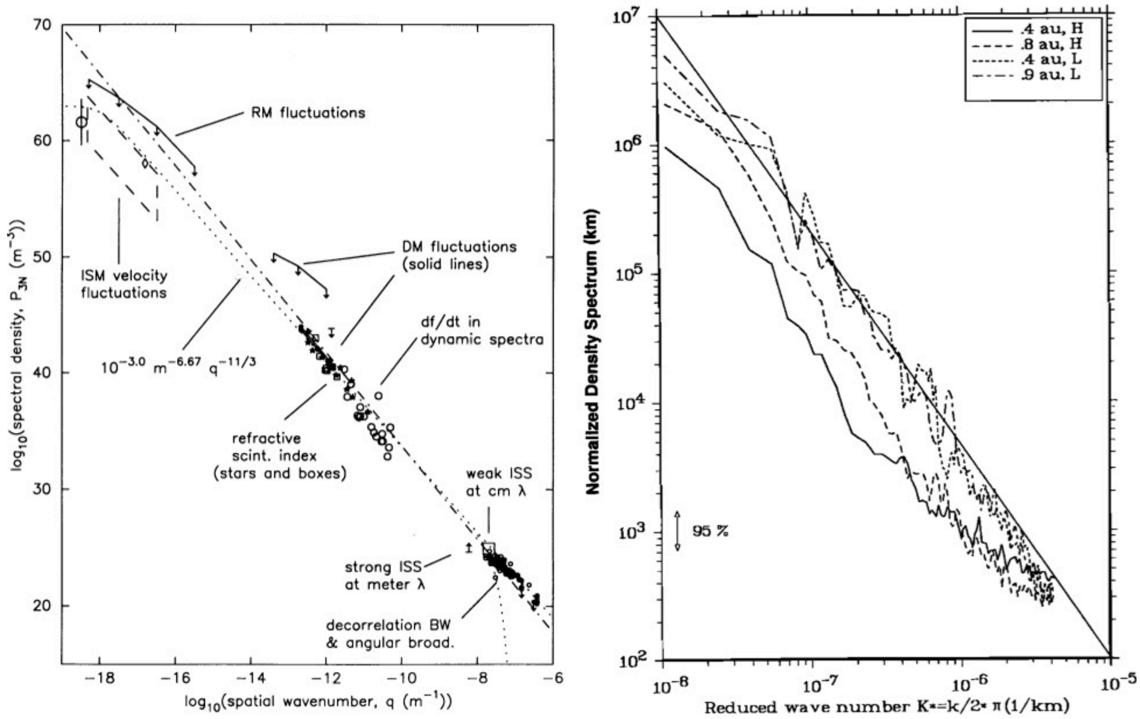

Figure 1.7: Density fluctuation spectra in the interstellar medium (left, taken from [2]) and the solar wind (right, taken from [3]). These power law spectra span multiple decades, even at scales where these fluctuations are expected to be strongly damped.

separates timescales. The cyclotron motion may be assumed to be much faster than any timescale of interest in the system—this allows for reduced descriptions of kinetic plasmas, which are discussed further in Sec. 1.5 and appendix A.

1.4 Phase mixing in turbulent magnetized plasmas: Questions

In Secs. 1.1 and 1.2 we discussed how phase mixing and turbulent cascade dictate the turbulent characteristics of a plasma individually. It is however unclear, as to what happens to phase mixing in a nonlinear turbulent system. Understanding how phase mixing works in presence of turbulence is an important problem in kinetic plasma turbulence.

A simple way to incorporate phase mixing in a model for a turbulent plasma would be to introduce it as a sink of energy to small velocity scales, at each spatial scale, in essence superimposing phase mixing on to the turbulent cascade [23–25]. For the cascade of a macroscopic quantity like density fluctuations, this would show up as a scale-by-scale dissipative term, where the rate of dissipation is proportional to the parallel wavenumber. Such dissipation would violate the constant-flux-through-scales assumption of Kolmogorov. Extraction of energy at each scale at a rate proportional to the wavenumber would imply that the energy spectrum should be an exponential decay instead of a power law. However, power law energy spectra are commonly observed in weakly collisional turbulent magnetized plasmas. A striking example is that of compressive fluctuations in astrophysical systems. Electron density fluctuations in the interstellar medium extend over twelve decades of scales, famously known as "the Great Power Law in the Sky" [2, 26, 27]. In the solar wind, these fluctuations are observed for roughly three decades [3, 28–37] (see Fig. 1.7). These observations are at scales where the plasma is weakly collisional. Linear theory predicts that compressive fluctuations should be strongly damped in the weakly collisional limit [38], which makes these observed power law spectra surprising. This suggests that when the system is nonlinear, the linear predictions need to be modified. A possible explanation for such power law spectra, though not specifically for these plasmas, was given recently by Plunk *et al.* [39, 40], where they argue that phase mixing is suppressed due to what is in essence, an "impedance mismatch" with the nonlinear turbulent frequency. However, in their study, they do not include the nonlinear cascade. Instead, they consider a single Fourier mode, and add a random source term as a stand-in for turbulence—this approach is quite different from the one we adopt here.

In this thesis, the interplay between the nonlinear cascade and phase mixing is studied. This is done by considering nonlinear models which incorporate both these effects[§]. The first nonlinear model allows for a turbulent cascade in the direction perpendicular to the guide field, but does not allow for a transfer of energy to small spatial scales parallel to the background field. In this scenario, when the turbulent cascade rate is comparable to or larger than the phase mixing rate, energy gets swept up to small spatial scales before it can phase mix. As a result a fluid-like turbulent cascade, *i.e.* a power law spectrum is observed. In the other, more interesting model, where the turbulent cascade proceeds in both perpendicular and parallel directions, a turbulent analog of the plasma echo is observed, which unravels the velocity space structure generated by phase mixing. This *stochastic plasma echo* suppresses phase mixing, which again results in a fluid-like turbulent cascade at scales where, in the linear limit, perturbations would be strongly damped due to phase mixing. Hence, regardless of whether or not there is a parallel cascade, power law energy spectra are observed for turbulent fluctuations at these "kinetic" scales.

[§] This is different from what is generally referred to as nonlinear Landau damping (see [41] and references therein for a detailed analysis of this problem from a mathematician's perspective) in the literature. The question there is what happens to the validity of Landau's results if the perturbations have finite amplitudes. In our work, all perturbations are assumed small compared to the equilibrium.

1.5 Kinetic Reduced MHD

1.5.1 Basic framework

The basic mathematical framework used in this work is known as Kinetic Reduced MagnetoHydroDynamics (KRMHD). KRMHD is the long wavelength limit of gyrokinetics [1, 17, 42–51]. It is derived in thorough detail in Schekochihin *et al.* [1], by expanding "δf gyrokinetics" in small $k_\perp \rho_i$ ($k_\perp$ is the perpendicular wavenumber, ρ_i is the ion Larmor radius). In this limit, the Alfvénic component of the cascade decouples from the compressive fluctuations. The dynamics of the system are completely determined by the Alfvénic fluctuations, which evolve according to reduced MHD [52, 53]. The compressive fluctuations, on the other hand, are described by a kinetic equation for a passive scalar that is nonlinearly advected by the background Alfvénic turbulence. These equations provide an efficient framework within which one may study the turbulent cascade of density and field strength fluctuations in weakly collisional turbulent magnetized plasmas like the solar wind.

The passive nature of compressive fluctuations in this model neatly ties in with a popular approach used to study turbulent cascade in fluid systems, namely that of passive scalar turbulence [14, 54–78]. This gives us the opportunity to study the general problem of *kinetic* passive scalar turbulence, while having a physically relevant system to compare with. General results regarding kinetic passive scalar turbulence are presented in Chapters 3, 4 and 5, by considering simplified versions of KRMHD. The full KRMHD equations are numerically solved in Chapter 6.

The derivation of KRMHD given in Schekochihin *et al.* [1] is extremely detailed, and we do not attempt to better it in this thesis. Instead, we give an outline of the derivation of KRMHD in appendix A, and give a summary of the final equations here.

The KRMHD model assumes a homogeneous equilibrium, with a Maxwellian as the background distribution function. A perturbation of this equilibrium is evolved in time. The Alfvén cascade is described by reduced MHD, which in its simplest form is written in terms of Elsasser variables [79]:

$$\frac{\partial \nabla_\perp^2 \xi^\pm}{\partial t} \mp v_A \frac{\partial \nabla_\perp^2 \xi^\pm}{\partial z} = -\frac{1}{2}\left[\{\xi^+, \nabla_\perp^2 \xi^-\} + \{\xi^-, \nabla_\perp^2 \xi^+\} \mp \nabla_\perp^2 \{\xi^+, \xi^-\}\right], \quad (1.16)$$

where the background magnetic field $\mathbf{B}_0 = B_0\hat{\mathbf{z}}$ is in the $\hat{\mathbf{z}}$ direction, $\hat{\mathbf{x}}$ and $\hat{\mathbf{y}}$ are the transverse directions, $\xi^\pm = \Phi \pm \Psi$, $v_A = B_0/\sqrt{4\pi m_i n_{0i}}$ is the Alfvén velocity, and Φ and Ψ are stream and flux functions respectively, which are related to the electrostatic potential (φ) and the magnetic vector potential ($A_\parallel$) by:

$$\Phi = \frac{c}{B_0}\varphi, \quad \Psi = -\frac{A_\parallel}{\sqrt{4\pi m_i n_{0i}}}, \quad (1.17)$$

where c is speed of light, m_i is the ion mass, and n_{0i} is the background ion density. The braces denote the Poisson bracket:

$$\{P, Q\} = \frac{\partial P}{\partial x}\frac{\partial Q}{\partial y} - \frac{\partial P}{\partial y}\frac{\partial Q}{\partial x}. \quad (1.18)$$

The left hand side of Eq. (1.16) describes Alfvén wave packets, traveling up or down the field line. The nonlinear interaction between these wave packets is captured by the right hand side. Observe that only counter-propagating Alfvén waves interact nonlinearly; these counter-propagating Alfvén waves give rise to the turbulent cascade by transferring energy to smaller spatial scales.

The compressive fluctuations are described in terms of two Elsasser-like variables g^+ and g^-:

$$\frac{dg^{\pm}}{dt} + v_\parallel \nabla_\parallel g^{\pm} = \frac{v_\parallel F_0(v_\parallel)}{\Lambda^{\pm}} \hat{\mathbf{b}} \cdot \nabla \int dv_\parallel g^{\pm}, \tag{1.19}$$

where $F_0(v_\parallel) = \exp(-v_\parallel^2/v_{\rm th}^2)/\sqrt{\pi}v_{\rm th}$ is a one-dimensional Maxwellian ($v_{\rm th} = \sqrt{2T_i/m_i}$ is the thermal velocity of ions, T_i is the ion temperature, m_i is the ion mass), and

$$\Lambda^{\pm} = -\frac{\tau}{Z} + \frac{1}{\beta_i} \pm \sqrt{\left(1 + \frac{\tau}{Z}\right)^2 + \frac{1}{\beta_i^2}}, \tag{1.20}$$

where τ is the ion to electron temperature ratio, Z is the ion charge in units of the electron charge, and $\beta_i = 8\pi n_{0i} T_i / B_0^2$ is the ion plasma beta. We observe from Eq. (1.20), that the range of $\Lambda^{\pm}$ is restricted to: $\Lambda^+ > 1$, and $\Lambda^- < 0$. The derivatives d/dt and $\nabla_\parallel$ in Eq. (1.19) are convective derivatives:

$$\frac{d}{dt} = \frac{\partial}{\partial t} + \{\Phi, \ldots\}, \quad \nabla_\parallel = \frac{\partial}{\partial z} + \frac{1}{v_A}\{\Psi, \ldots\}. \tag{1.21}$$

The relationship between the perturbed ion distribution function and $g^{\pm}$ is given in appendix A (see Eqs. (A.35) and (A.38)). Eqs. (1.16) and (1.19) together constitute the KRMHD model.

1.5.2 Conserved quantities

The energies in each of the Elsasser variables $(\xi^{\pm}, g^{\pm})$ are conserved independently in KRMHD:

$$W = W_{\mathrm{AW}}^{+} + W_{\mathrm{AW}}^{-} + W_{\mathrm{compr}}^{+} + W_{\mathrm{compr}}^{-}, \tag{1.22}$$

where

$$W_{\mathrm{AW}}^{\pm} = \int d^3\mathbf{r} \frac{m_i n_{0i}}{2} \left|\nabla_{\perp}\xi^{\pm}\right|^2 \tag{1.23}$$

are energies of the right and left-going Alfvénic fluctuations, and

$$W_{\mathrm{compr}}^{\pm} = \int d\mathbf{r} \frac{n_{0i}T_{0i}}{2} \left[\int dv_{\parallel} \frac{\left(g^{\pm}\right)^2}{F_0} - \frac{1}{\Lambda^{\pm}} \left(\int dv_{\parallel} g^{\pm}\right)^2\right] \tag{1.24}$$

are energies of the $+$ and $-$ components of the compressive fluctuations[¶], as defined in the previous section, respectively; W is the total free energy.

[¶]Both the terms in Eq. (1.24) are positive for the "$-$" mode, since $\Lambda^{-} < 0$. For the "$+$" mode, W_{compr}^{+} can be shown to be positive using Cauchy-Schwarz inequality, and the condition $\Lambda^{+} > 1$.